Liquid Crystals
Publication details, including instructions for authors and subscription information:
http://www.informaworld.com/smpp/title~content=t713926090

Relaxation from transient and stationary states in the deformed aligned phase (DAP) effect in quasi-homeotropic liquid crystal layers

S. Frunză[a]; T. Beica[a]; R. Moldovan[a]; M. Giurgea[a]; F. Cotorobai[b]
[a] Institute of Physics and Technology of Materials, Bucharest-Magurele, Romania [b] Institute of Nuclear Physics and Engineering, Bucharest-Magurele, Romania

To cite this Article Frunză, S. , Beica, T. , Moldovan, R. , Giurgea, M. and Cotorobai, F.(1988) 'Relaxation from transient and stationary states in the deformed aligned phase (DAP) effect in quasi-homeotropic liquid crystal layers', Liquid Crystals, 3: 2, 285 — 297
To link to this Article: DOI: 10.1080/02678298808086375
URL: http://dx.doi.org/10.1080/02678298808086375

LIQUID CRYSTALS, 1988, VOL. 3, NO. 2, 285–297

Relaxation from transient and stationary states in the deformed aligned phase (DAP) effect in quasi-homeotropic liquid crystal layers

by S. FRUNZĂ, T. BEICA, R. MOLDOVAN and M. GIURGEA
Institute of Physics and Technology of Materials, Bucharest–Magurele, MG-7, Romania

and F. COTOROBAI
Institute of Nuclear Physics and Engineering, Bucharest–Magurele, MG-6, Romania

(*Received 2 October 1986; accepted 12 August 1987*)

The relaxation of the molecular orientation in the DAP effect has been studied experimentally after removal of the electric field, for different values of the applied field and for three quasi-homeotropic initial geometries. The main aspects of the relaxation process are obtained by numerical integration of the Ericksen–Leslie equations with suitable boundary conditions.

1. Introduction

In the electro-optical field effects used in liquid crystal displays, the order of magnitude of the decay times is 100 ms, depending on the cell thickness and temperature and on the particular liquid crystal material. Much shorter decay times (~ 5 ms) are mentioned by Labrunie *et al.* [1] for cells addressed with high voltages (about 100 V) for very short times. These observations showed that the relaxation from a transient state may be appreciably more rapid than from a stationary one.

This suggested to us that it would be worth comparing the relaxation mechanism from transient states with that from stationary states. The relaxation of the orientation of the director in nematic liquid crystals have been calculated on the basis of the continuum theory [2, 3]. The Ericksen–Leslie hydrodynamic equations were solved by numerical integration [4, 5], as well as by an infinite series method [6]. These theoretical treatments explain the behaviour of the liquid crystal and especially the 'bounce' observed in light transmission versus time. In these papers the relaxation from a steady state of the orientational distortion was investigated. We intended to compare, both by experiment and by theory, the relaxation from transient and stationary states. The results in figure 1 demonstrate the outstanding differences in the relaxation behaviour between these two states. In this figure the oscillographic traces record the electro-optic response of a cell for deformed aligned phases (DAPs) to the application and interruption of the electric field. The cell is placed between crossed polarizers, oriented at 45° to the plane containing the director during its rotation. The continuous curve is generated by applying a voltage which is interrupted after a stationary state is reached. The value of this voltage is chosen so that the induced transmission of the cell corresponds to the first maximum in the curve of transmission versus voltage for the stationary states. The rising and decaying parts of the curve show the transmission during the application and after the interruption of the electric field. The time-base

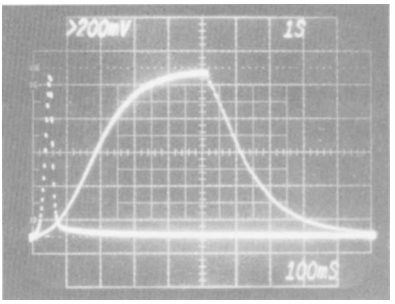

Figure 1. Oscillograph traces of the electro-optic response for a cell with a-type geometry (see figure 2). The continuous curve was generated by applying the voltage until the stationary state is reached; relaxation occurs from this state. The dotted curve was generated by interrupting the voltage before the stationary state was reached; relaxation occurs from this transient state.

for the rising and decaying parts is 1 and 0·1 s per division, respectively. The dotted curve shows the cell transmission when the applied voltage, about three times higher, is interrupted before reaching the stationary state; that is, when the transmission corresponds also to the first maximum in the curve of transmission versus voltage. For this last curve the time-base is 0·1 s per division for both the rising and the decaying part. It is clear that the relaxation from the transitory state takes place much more rapidly (dotted curve) than from the stationary state (continuous curve).

The aim of this paper is to establish the distortion state of the molecular orientation corresponding to a given optical phase difference on removal of the electric field, the distortion being inferred from the mode of relaxation after the interruption of the electric field. In particular we wish to establish the dependence of this distortion on the inclination of the molecular orientation at the cell walls.

2. Experimental

The experimental cells were made from two plane-parallel glass plates, 3 mm thick, coated with transparent layers of tin oxide. The quasi-homeotropic orientation was obtained by combining the effect of a silicon oxide (SiO) layer about 15 nm thick, deposited at an angle of incidence greater than 80°, and that of the dopant for homeotropic orientation contained in the liquid crystal material (997 Merck, with negative dielectric anisotropy). The 8 μm thickness of the liquid crystal layer was set by inserting Mylar spacers. The experiments were performed on three types of cell with homeotropic alignment (see figure 2):

(*a*) normal orientation at one of the surfaces (obtained without SiO deposition) and tilted orientation at the other surface,
(*b*) symmetrical, tilted orientation on both surfaces and
(*c*) asymmetrical, tilted orientation on both surfaces.

The experimental set-up for measuring the electro-optic response of the cell is sketched in figure 3. The addressing voltage of the cell is provided by the generator G which produces square waves, unipolar pulses, of adjustable frequency (which provide the frequency of the alternating applied voltage) together with a pulse generator, which determines the length of the pulse train, and a device based on the two input pulses, which gives at the output trains of square waves, alternating pulses of adjustable length and frequency, applied to the cell.

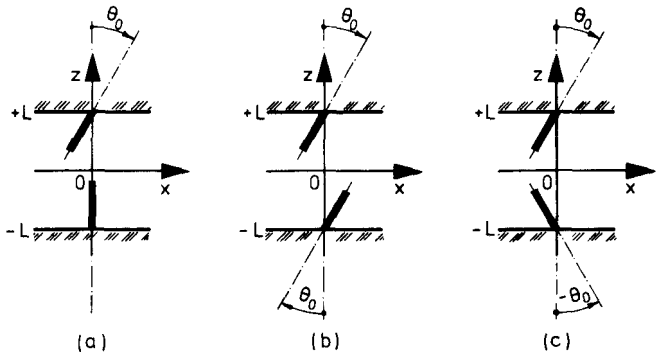

Figure 2. The quasi-homeotropic geometries of the liquid crystal cells investigated; θ_0 is the angle between the director and the z axis at the surfaces.

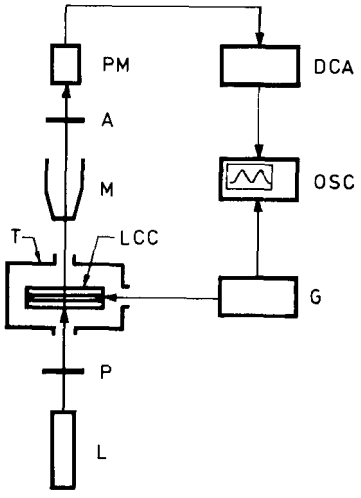

Figure 3. Experimental set-up. The liquid crystal cell (LCC) is placed in a chamber (T) thermically stabilized with an accuracy of 0·2°C, put on the stage of a polarizing microscope (M) provided with polarizers A and P. A He–Ne laser (L) is the source of monochromatic light. The light transmitted by the cell is received by the photomultiplier PM (RCA, 1 P 28 type), the photoelectric signal being amplified by a d.c. amplifier (DCA) and recorded on a memory oscilloscope. The addressing voltage is provided by the generator G.

3. Experimental results

The experimental results for the dynamics of the relaxation of the molecular orientation for the a, b and c type cells are shown in figures 4, 5 and 6, respectively. The plots show $-\ln[(\varphi - \varphi_0)/(\varphi_i - \varphi_0)]$ versus time measured from the moment when the electric field was turned off. We denote by φ the phase difference introduced by the cell between the ordinary and the extraordinary light beams at a time during the relaxation after the removal of the electric field, and by φ_i the maximum value of the phase difference obtained by the application of the electric field. Because of the tilted anchoring at the glass surfaces, the cell introduces a non-zero phase difference φ_0, even in the absence of the electric field. For the evaluation of the phase differences introduced by the cell, we have used the relation

$$I = I_0 \sin^2(\varphi/2),$$

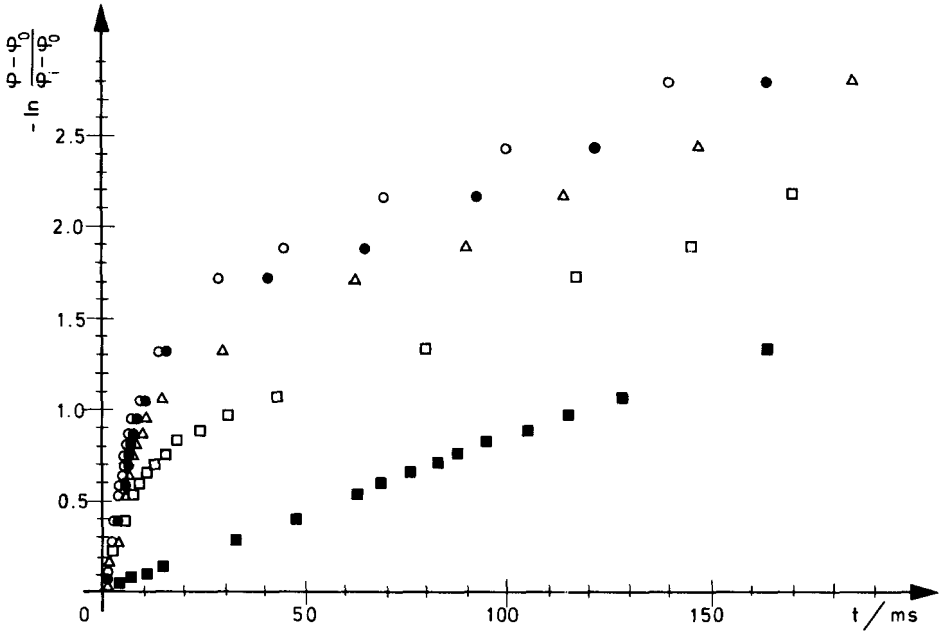

Figure 4. Experimental relaxation curves for the a-type geometry. ○, $-U = 48{\cdot}3$ V, $t_a =$ 2 ms; ●, $-U = 32{\cdot}5$ V, $t_a = 5$ ms; △, $-U = 25{\cdot}5$ V, $t_a = 10$ ms; □, $-U = 21{\cdot}2$ V, $t_a = 20$ ms; ■, $-U = 7{\cdot}1$ V, relaxation from the stationary state.

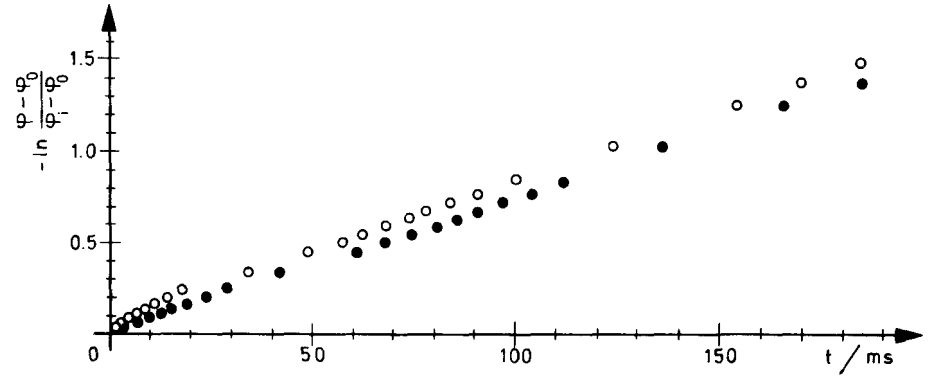

Figure 5. Experimental relaxation curves for the b-type geometry. ○, $-U = 54{\cdot}5$ V, $t_a = 2$ ms; ●, $-U = 6{\cdot}4$ V, relaxation from the stationary state.

where I denotes the intensity and I_0 the maximum intensity of the light transmitted by the system. The ratio I/I_0 was evaluated from the trace on the memory oscilloscope screen.

Oscilloscope traces were made for each geometry and for different values of the applied voltage, lasting sufficiently long for the relaxation to begin from the same φ_i value (for example, that corresponding to 90% transmission after passing the first maximum value in the transmission versus voltage curve).

The values of the applied voltages and the times t_a for which the voltages were applied are indicated in the caption of each figure. The relaxation curves in figure 4 for a-type geometry display two linear parts, the first with a large slope (fast relaxation) joined at longer times by a linear part of smaller slope (slow relaxation). The exception

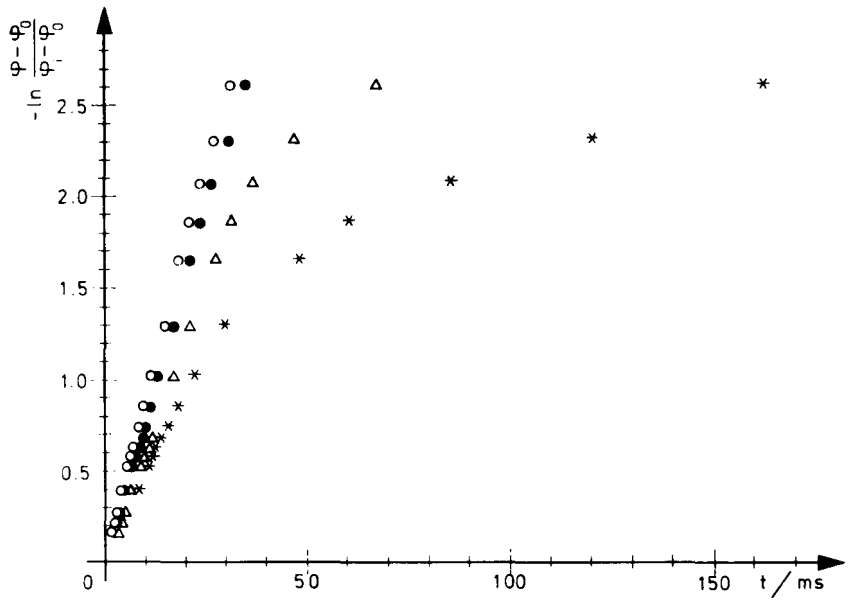

Figure 6. Experimental relaxation curves for the c-type geometry. ○, $-U = 45{\cdot}7$ V, $t_a = 2$ ms; ●, $-U = 23{\cdot}7$ V, $t_a = 10$ ms; △, $-U = 15{\cdot}2$ V, $t_a = 50$ ms; ∗, $-U = 13{\cdot}8$ V, $t_a = 100$ ms.

is the curve for relaxation from the equilibrium (stationary) state, which displays only the slow relaxation type of curve. Note that this straight line is parallel to the linear part, corresponding to longer relaxation times of the other curves. The exponential decay of the phase difference, shown by the existence of the straight parts of the curve, has a time constant of ~ 120 ms for slow relaxation and 10 ms for fast relaxation.

For a cell of b-type geometry the transmission curves from both the stationary and the transient states versus applied voltage are shown in figure 5. For this geometry the relaxation is nearly all of the slow type, with the same time constant as the slow relaxation for a-type geometry.

Figure 6 shows that for c-type geometry the relaxation is mainly of the fast type, with a time constant between 10 and 20 ms, followed after a long time by relaxation of the slow type, with a time constant of, again, ~ 120 ms. For this geometry, if the voltage is applied for a longer time the director begins to leave the xz plane, which is determined by the treatment of the glass plates.

4. Theoretical approach

To calculate the distribution of the molecular orientation produced by applying an electric field and its evolution after turning off of the field, we use Ericksen–Leslie theory [2, 3]. This theory gives the equations for the vector fields that describe the flow of a nematic liquid crystal, demonstrating the hydrodynamic movement induced by the back-flow, as well as the reverse effect of modification of the molecular orientation by flow velocity gradients.

Let us consider a film of a nematic liquid crystal with dielectric anisotropy $\varepsilon_a = \varepsilon_\parallel - \varepsilon_\perp < 0$, of thickness $2L$, bounded by two plane, parallel surfaces. We refer this film to a set of cartesian axes with the origin in its middle plane and with the Oz axis normal to the planar boundaries of the film. We denote by θ the angle between

the director **n** and the Oz axis. Assuming that during the rotation of the molecules the director remains in a plane parallel to xz, that the fluid velocity **v** has a non-zero component only in the Ox direction, and that **n** and **v** are functions of z and of time t only, we can write

$$\mathbf{n} = [\sin\theta(z,t), 0, \cos\theta(z,t)], \tag{1}$$

and

$$\mathbf{v} = [u(z,t), 0, 0]. \tag{2}$$

For the application of a voltage U to the liquid crystal film, generating an electric field in the Oz direction, and in the absence of a body force and neglecting inertial effects, the resulting equation (from the law of conservation of linear momentum) is, in the Ericksen–Leslie theory,

$$\frac{\partial}{\partial z}\left\{(\mu_2\cos^2\theta - \mu_3\sin^2\theta)\dot{\theta} + \tfrac{1}{2}[2\mu_1\sin^2\theta\cos^2\theta + (\mu_3 + \mu_6)\sin^2\theta + (\mu_5 - \mu_2)\cos^2\theta + \mu_4]\frac{\partial u}{\partial z}\right\} = 0. \tag{3}$$

The equation resulting from the law of conservation of angular momentum is

$$\lambda_1\dot{\theta} - (k_{33} - k_{11})\sin\theta\cos\theta\left(\frac{\partial\theta}{\partial z}\right)^2 + \tfrac{1}{2}[\lambda_2 - \lambda_1 - 2\lambda_2\sin^2\theta]\frac{\partial u}{\partial z} + (k_{33}\cos^2\theta + k_{11}\sin^2\theta)\frac{\partial^2\theta}{\partial z^2} - (U^2\varepsilon_a\sin\theta\cos\theta) \times \left\{(\varepsilon_\perp + \varepsilon_a\cos^2\theta)^2\left[\int_{-L}^{L}\frac{\mathrm{d}z}{(\varepsilon_\perp + \varepsilon_a\cos^2\theta)}\right]^2\right\}^{-1} = 0. \tag{4}$$

Here we have used Chandrasekhar's [7] notation for the viscosity coefficients μ_i ($i = 1, \ldots, 6$):

$$\lambda_1 = \mu_2 - \mu_3, \qquad \lambda_2 = \mu_5 - \mu_6,$$

and k_{11}, k_{22} and k_{33} are the splay, twist and bend elastic coefficients.

In order to obtain dimensionless equations, we make the following substitutions:

$$\eta = \frac{z}{L}, \qquad s = -\frac{k_{33}}{\lambda_1 L^2}t, \qquad v = -\frac{L\lambda_1}{k_{33}}u, \qquad \varepsilon = \frac{\varepsilon_a}{\varepsilon_\perp}.$$

We also introduce the notations

$$U_0 = \pi\left(\frac{k_{33}}{-\varepsilon_a}\right)^{1/2},$$

$$f_1(\theta) = -\frac{\mu_2}{\lambda_1} + \frac{\mu_2 + \mu_3}{\lambda_1}\sin^2\theta,$$

$$f_2(\theta) = \frac{\mu_4 + \mu_5 - \mu_2}{2\lambda_1} + \frac{2\mu_1 + \mu_2 + \mu_3 - \mu_5 + \mu_6}{2\lambda_1}\sin^2\theta - \frac{\mu_1}{\lambda_1}\sin^4\theta,$$

$$f_3(\theta) = \frac{\lambda_2 - \lambda_1}{2\lambda_1} - \frac{\lambda_2}{\lambda_1}\sin^2\theta,$$

$$f_4(\theta) = 1 - \frac{k_{33} - k_{11}}{k_{33}} \sin^2\theta,$$

$$f_5(\theta) = -\frac{k_{33} - k_{11}}{k_{33}} \sin\theta\cos\theta,$$

$$T(\theta) = \left(\frac{U}{U_0}\right)^2 \pi^2 \sin\theta\cos\theta \left[(1 + \varepsilon\cos^2\theta)^2 \left(\int_{-1}^{1} \frac{d\eta}{1 + \varepsilon\cos^2\theta}\right)^2\right].$$

In this notation, equations (3) and (4) become

$$\frac{\partial}{\partial\eta}\left[f_1(\theta)\frac{\partial\theta}{\partial s}\right] - \frac{\partial f_2}{\partial\eta}\frac{\partial\theta}{\partial\eta}\frac{\partial v}{\partial\eta} - f_2(\theta)\frac{\partial^2 v}{\partial\eta^2} = 0 \tag{5}$$

and

$$\frac{\partial\theta}{\partial s} = f_4(\theta)\frac{\partial^2\theta}{\partial\eta^2} + f_5(\theta)\left(\frac{\partial\theta}{\partial\eta}\right)^2 - f_3(\theta)\frac{\partial v}{\partial\eta} + T(\theta), \tag{6}$$

respectively.

In order to obtain the pattern of molecular orientations and the distribution of velocities when the electric field is applied and after it is turned off, we numerically integrated the system of equations (5) and (6). For this purpose the derivatives with respect to η and s were replaced by finite difference quotients. In the derivatives with respect to η central differences were used, while for the derivatives with respect to s forward differences were used. In order to solve equations (5) and (6), in which finite differences were introduced, an implicit triangulation scheme [8] was used, and to start the numerical integration we began with equation (6). In order to ensure the linearity of the algebraic equations giving the values of θ in the space–time lattice points, all nonlinear expressions in θ on the right-hand side of these equations were taken for the left extremity of each time step. The calculations were performed on an IBM 370/135 computer.

With the assumption of strong anchoring, using the dimensionless variables η and s, we have for the three geometries shown in figure 2 the boundary condition

$$v(\pm 1, s) = 0.$$

In addition, we have for the a-type geometry

$$\left.\begin{aligned}\theta(-1,s) &= 0,\\ \theta(+1,s) &= \theta_0;\end{aligned}\right\} \tag{7a}$$

for the b-type geometry

$$\left.\begin{aligned}\theta(-1,s) &= \theta_0,\\ \theta(+1,s) &= \theta_0;\end{aligned}\right\} \tag{7b}$$

and for the c-type geometry

$$\left.\begin{aligned}\theta(-1,s) &= -\theta_0,\\ \theta(+1,s) &= \theta_0.\end{aligned}\right\} \tag{7c}$$

We have adopted the simplifying assumption that, before the application of the electric field, θ changes linearly with η from one surface to the other.

We wished to test by computation the experimental results (see figures 4–6) which show the influence of the cell geometry and of the value of the applied voltage on the type of relaxation. We have calculated the phase differences φ introduced by a liquid crystal film crossed at normal incidence by a monochromatic light beam of wavelength λ. This phase difference was evaluated from

$$\varphi(s) = \frac{2\pi n_o L}{\lambda} \int_{-1}^{1} \{[1 - \nu \sin^2 \theta(\eta, s)]^{-1/2} - 1\} \, d\eta. \tag{8}$$

Here

$$\nu = \frac{n_e^2 - n_o^2}{n_o^2},$$

with n_e, n_o denoting the extraordinary and ordinary refractive indices for the wavelength, $\lambda = 0{\cdot}5\,\mu m$.

The literature does not contain all the material constants for the 997 Merck liquid crystal, which are necessary for the calculations. So, in order to compare qualitatively the shape of the experimental relaxation curves with those from theory, we have used some of the constants for MBBA which we consider to be convenient to our purpose. The material constants were given the values $n_o = 1{\cdot}50$, $n_e = 1{\cdot}78$, $\varepsilon_{\parallel} = 4{\cdot}7$ and $\varepsilon_{\perp} = 5{\cdot}4$. We used values from [9] for the elastic constants k_{ii}, and values from [10] for the viscosity coefficients μ_i, which are denoted by α_i in [10]. Also,

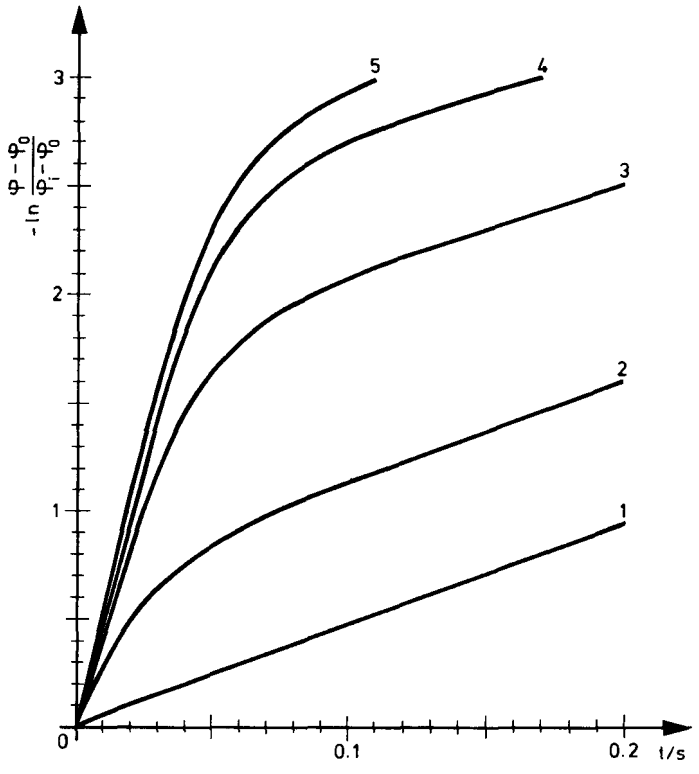

Figure 7. Computed relaxation curves for the a-type geometry; $\theta(-1; s) = 0°$, $\theta(+1; s) = 5°$. Curve 1, $U/U_0 = 1{\cdot}5$; curve 2, $U/U_0 = 2{\cdot}5$; curve 3, $U/U_0 = 3$; curve 4, $U/U_0 = 5$; curve 5, $U/U_0 = 10$.

we chose

$$L = 5\,\mu\text{m}, \qquad \theta_0 = 5°. \tag{9}$$

In the computation, the applied voltage was assumed to be interrupted when $\varphi - \varphi_0$ reached the predetermined value of π, and as initial value φ_i we adopted the maximum value reached after the field was turned off. Due to the interaction between the hydrodynamic movement and the rotation of the director, the phase difference φ can grow a little more immediately after removal of the electric field.

In figures 7–9 we have plotted computed values of $-\ln[(\varphi - \varphi_0)/(\varphi_i - \varphi_0)]$ versus s for the three geometries, adopting the values (9) for L and θ_0. The chosen

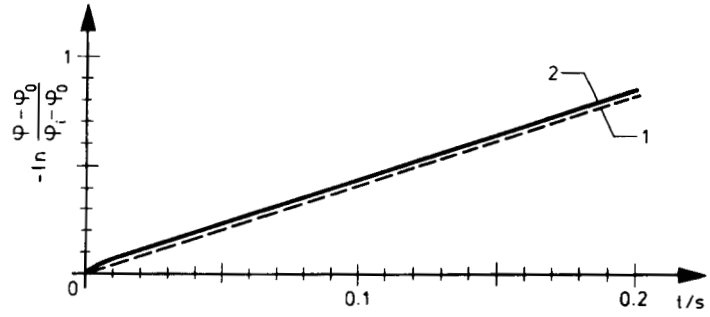

Figure 8. Computed relaxation curves for the b-type geometry; $\theta(-1;s) = 5°$, $\theta(+1;s) = 5°$. Curve 1, $U/U_0 = 1{\cdot}5$; curve 2, $U/U_0 = 10$.

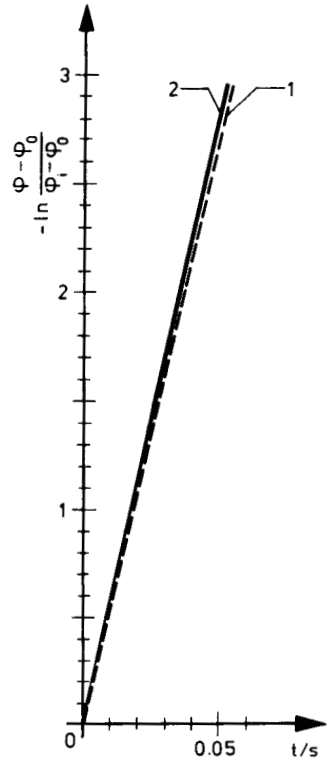

Figure 9. Computed relaxation curves for the c-type geometry; $\theta(-1;s) = -5°$, $\theta(+1;s) = +5°$. Curve 1, $U/U_0 = 3$; curve 2, $U/U_0 = 5$.

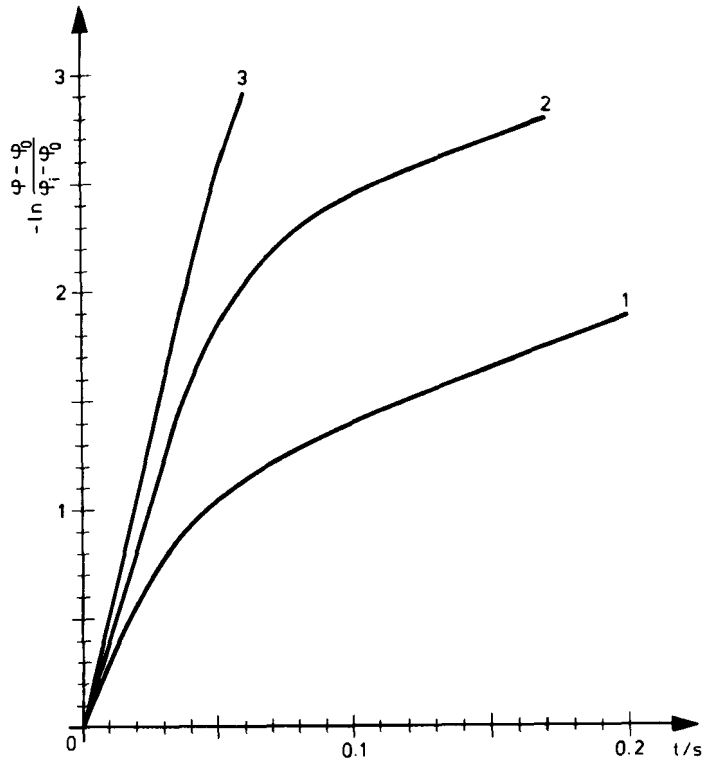

Figure 10. Computed relaxation curves for the c-type geometry; $\theta(-1;s) = -3°$, $\theta(+1;s) = +7°$. Curve 1, $U/U_0 = 2{\cdot}1$; curve 2, $U/U_0 = 2{\cdot}5$; curve 3, $U/U_0 = 10$.

value U/U_0, as a parameter, is shown for each curve. Figure 10 is for the c-type geometry and the boundary conditions

$$\theta(-1,s) = -3°, \qquad \theta(+1,s) = +7°. \tag{10}$$

In figure 11 the variation of the distortion angle θ throughout the thickness of the liquid crystal layer is given for $U/U_0 = 1{\cdot}5$, $2{\cdot}5$, 5 and 10, for the a-type geometry. The variation of the flow speed v is shown in figure 12 for the same geometry and the same U/U_0 values, also at $s = 0$. For the low voltage ($U/U_0 = 1{\cdot}5$) the curve for θ is predominantly symmetric about the mid-plane of the cell, and the curve for v shows opposite direction flows in the neighbourhood of the two boundaries. For higher voltages the curve for θ becomes more and more asymmetric, with flows in almost the same direction throughout the liquid crystal layer. In the b-type geometry the computed curve of the orientations is symmetric relative to the mid-plane for any value of the ratio U/U_0, and the curve of the flow speed is asymmetric.

The computations for the c-type geometry with the conditions (7 *c*) and (9) give an asymmetric curve of θ for any value of U/U_0 and the same direction of flow throughout the thickness of the cell. Computed curves for the distortion angle θ and the flow speed v for the b-type and c-type geometries, comprising six pages have been deposited as a Supplementary Publication with the British Library Document Supply Centre. Copies of these patterns may be obtained by using the procedure described at the end of this issue and by quoting SUP 1650.

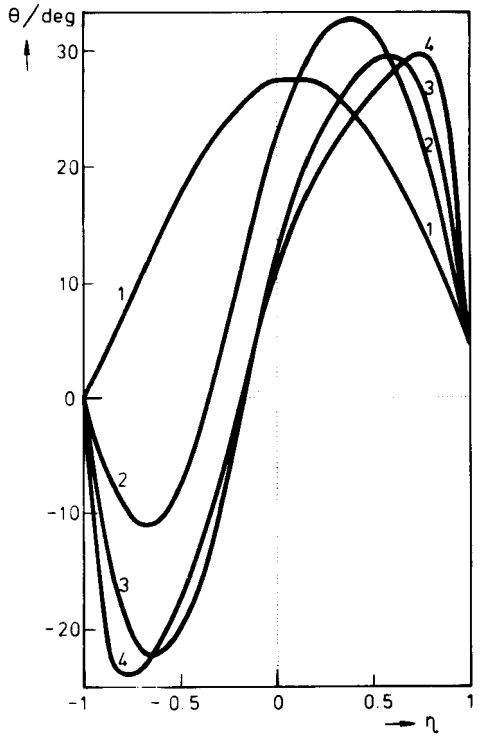

Figure 11. Computed pattern of the molecular orientation angle, θ, on removal of the electric field for the a-type geometry. Curve 1, $U/U_0 = 1{\cdot}5$; curve 2, $U/U_0 = 2{\cdot}5$; curve 3, $U/U_0 = 5$; curve 4, $U/U_0 = 10$.

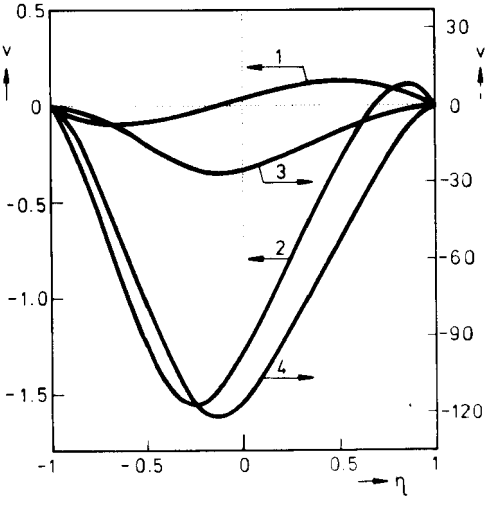

Figure 12. Computed pattern of the flow speed, v, on removal of the electric field for the a-type geometry. Curve 1, $U/U_0 = 1{\cdot}5$; curve 2, $U/U_0 = 2{\cdot}5$; curve 3, $U/U_0 = 5$; curve 4, $U/U_0 = 10$.

We note from figure 11 that, on increasing the applied voltage, the molecular orientation curves become more and more asymmetric. We wished to see how such a curve might change by increasing the time during which the voltage is applied. We therefore calculated the molecular orientation angle θ for an a-type geometry cell and for $U/U_0 = 2{\cdot}5$, for phase differences $\varphi - \varphi_0$ introduced by the cell of π, 3π and 6π. The results of these calculations are shown in figure 13. We can see from this figure that, by increasing the time for which the voltage is applied, and so approaching the stationary state, the orientational distribution curve changes from a predominantly asymmetric shape towards a predominantly symmetric form. As expected, we obtained a slow-type relaxation curve by turning off the voltage when a stationary state (such as that corresponding to curve 3 in figure 13) was almost reached.

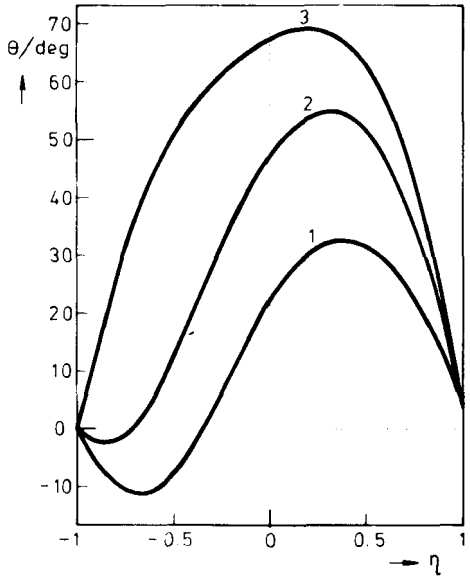

Figure 13. Computed pattern of the molecular orientation angle, θ, for an a-type geometry cell with $U/U_0 = 2{\cdot}5$, when the phase difference $\varphi - \varphi_0$ introduced by the cell reached the values π (curve 1), 3π (curve 2) and 6π (curve 3).

5. Discussion

As we used the material constants of MBBA in the calculations, the comparison between the theoretical and experimental results is only qualitative. The similarity between the theoretical and experimental curves for the a-type geometry (see figures 7 and 4) and the b-type geometry (see figures 8 and 5) is therefore quite remarkable. For the c-type geometry the computations made with the conditions (7 *c*) and (9) predict only fast relaxation (see figure 9) for any applied voltage, while experimentally we have found (see figure 6) that at low voltages the initial fast relaxation is followed by a slow relaxation. Qualitative agreement between theory and experiment has also been obtained for the c-type geometry (see figure 10) by adopting different anchoring angles at the two boundary surfaces (condition (10)). It is impossible, experimentally, to fix the value of the angle θ_0, so that it is likely that the experimental results are obtained for cells with unequal absolute values of the anchoring angles at the two surfaces.

The slow-type relaxation is correlated with a symmetric pattern of the molecular orientation angle θ at the moment of the removal of the electric field (as for the b-type geometry or the a-type geometry for low voltages). In contrast, the fast-type relaxation is correlated with an asymmetric curve for the molecular orientation angle θ when the electric field is removed (as for the c-type geometry and the a-type geometry for high voltages).

The existence of a correlation between the relaxation type and the molecular orientation when the electric field is interrupted was also reported for DAP cells with liquid crystals of positive dielectric anisotropy. Bos and Koehler-Beran [11] showed that if the distribution of the molecular orientation angle θ was asymmetric relative to the mid-plane of the cell at the moment of removing the electric field (the case of π cells), the relaxation would be more rapid than for a symmetric distribution.

6. Conclusions

Despite all the approximations adopted, the computations of the relaxation curves from the Ericksen–Leslie equations allowed us to obtain the essential aspects of the observed relaxation phenomenon. The characteristic of the relaxation is determined by the molecular orientation distortion at the moment of removing the electric field. This distortion depends strongly on the molecular orientation distortion before the field is applied, and which is, in turn, determined by the molecular anchoring conditions at the two surfaces.

References

[1] LABRUNIE, G., ROBERT, J., and BOREL, J., 1974, *Appl. Optics*, **13**, 1355.
[2] ERICKSEN, J. L., 1961, *Trans. Soc. Rheol.*, **5**, 23.
[3] LESLIE, F. M., 1968, *Archs ration. Mech. Analysis*, **28**, 265.
[4] VAN DOORN, C. Z., 1975, *J. appl. Phys.*, **46**, 3738.
[5] BERREMAN, D. W., 1975, *J. appl. Phys.*, **46**, 3746.
[6] CLARK, M. G., and LESLIE, F. M., 1978, *Proc. R. Soc.* A, **361**, 463.
[7] CHANDRASEKHAR, S., 1977, *Liquid Crystals* (Cambridge University Press), Chap. 3.
[8] MARCHIUK, G. I., 1980, *Methods of Numerical Mathematical Analysis* (Nauka), Chap. 9 (in Russian).
[9] RONDELEZ, F., and HULIN, J. P., 1972, *Solid St. Commun.*, **10**, 1009.
[10] GÄHWILLER, C., 1971, *Phys. Lett.* A, **36**, 311.
[11] BOS, P. J., and KOEHLER-BERAN, K. R., 1983, *Japan Display*, p. 478.